Journal of Medicinal Chemistry Article

J. Med. Chem. **2009,** *52,* 8047–8056 **8047**
DOI: 10.1021/jm901260k

Carbamate Analogues of Fumagillin as Potent, Targeted Inhibitors of Methionine Aminopeptidase-2

Christopher C. Arico-Muendel,*[,†] Dennis R. Benjamin,[‡] Teresa M. Caiazzo,[§] Paolo A. Centrella,[†] Brooke D. Contonio, Charles M. Cook,[∥,⊥] Elisabeth G. Doyle,[#] Gerhard Hannig,[▽] Matthew T. Labenski,[○] Lily L. Searle,* Kenneth Lind,[†] Barry A. Morgan,[†] Gary Olson,[∥] Christopher L. Paradise,[◆] Christopher Self,*[,∥] Steven R. Skinner,[†] Barbara Sluboski,[∥] Jennifer L. Svendsen, Charles D. Thompson,[¶] William Westlin,[○] and Kerry F. White[+]

Praecis Pharmaceuticals, Inc., 830 Winter Street, Waltham, Massachusetts 02451-1420, Provid Research, 10 Knightsbridge Road, Piscataway, New Jersey 08854. [†]Present address: GlaxoSmithKline, 830 Winter Street, Waltham, MA 02451-1420. [‡]Present address: Seattle Genetics, Inc., 21823 30th Drive SE, Bothell, WA 98021. [§]Present address: Pfizer Research, One Burtt Road, Andover, MA 01810. [∥]Present address: Provid Pharmaceuticals, Inc., 671 U.S. Route 1, North Brunswick, NJ 089002. [⊥]Deceased August, 2008. [#]Present address: Vertex Pharmaceuticals, 130 Waverly Street, Cambridge, MA 02139. [▽]Present address: Ironwood Pharmaceuticals, 320 Bent Street, Cambridge, MA 02141. [○]Present address: Avila Therapeutics, 100 Beaver Street, Waltham, MA 02453. [◆]Present address: The University of Texas—Southwestern Medical Center, 5323 Harry Hines Boulevard, Dallas, TX 75390. [¶]Present address: Department of Drug Metabolism, Merck & Company Incorporated, West Point, PA. [+]Present address: Infinity Pharmaceuticals, 780 Memorial Drive, Cambridge, MA 02139.

Received August 21, 2009

Inhibition of methionine aminopeptidase-2 (MetAP2) represents a novel approach to antiangiogenic therapy. We describe the synthesis and activity of fumagillin analogues that address the pharmacokinetic and safety liabilities of earlier candidates in this compound class. Two-step elaboration of fumagillol with amines yielded a diverse series of carbamates at C6 of the cyclohexane spiroepoxide. The most potent of these compounds exhibited subnanomolar inhibition of cell proliferation in HUVEC and BAEC assays. Although a range of functionalities were tolerated at this position, α-trisubstituted amines possessed markedly decreased inhibitory activity, and this could be rationalized by modeling based on the known fumagillin-MetAP2 crystal structure. The lead compound resulting from these studies, (3*R*,4*S*,5*S*,6*R*)-5-methoxy-4-((2*R*,3*R*)-2-methyl-3-(3-methylbut-2-enyl)oxiran-2-yl)-1-oxaspiro[2.5]octan-6-yl (*R*)-1-amino-3-methyl-1-oxobutan-2-ylcarbamate, (PPI-2458), demonstrated an improved pharmacokinetic profile relative to the earlier clinical candidate TNP-470, and has advanced into phase I clinical studies in non-Hodgkin's lymphoma and solid cancers.

Introduction

Antineoplastic properties of the sesquiterpenoid natural product fumagillin ((2*E*,4*E*,6*E*,8*E*)-10-((3*R*,4*S*,5*S*,6*R*)-5-methoxy-4-((2*R*,3*R*)-2-methyl-3-(3-methylbut-2-enyl)oxiran-2-yl)-1-oxaspiro[2.5]octan-6-yloxy)-10-oxodeca-2,4,6,8-tetraenoic acid, **1**, Figure 1) were reported 50 years ago, but it was first characterized as an inhibitor of angiogenesis by Folkman's group in 1990.[1] Angiogenesis, the process of new blood vessel formation, has emerged as an attractive strategy for cancer therapy based on the observation that tumor growth was significantly limited in its absence. By selectively targeting proliferating endothelial cells that promote neovascularization in tumor tissue, this strategy appears to offer a means to circumvent the nonspecific toxicity of conventional chemotherapeutic drugs. Several angiogenesis inhibitors, having demonstrated efficacy in a number of in vivo models, have progressed through human clinical trials and gained FDA approval.[2] Two early clinical successes included the VEGF[a] receptor antagonists bevacizumab, which gained approval for nonsmall cell lung cancer and colorectal cancer, and pegaptanib, approved for age-related macular degeneration. Both drugs are macromolecules (an antibody and a pegylated aptamer, respectively); the first small-molecule approvals included sorafenib for renal cell carcinoma (RCC) and sunitinib for RCC and gastrointestinal stromal tumor. With the clinical validation of antiangiogenesis as a beneficial chemotherapeutic strategy in place, the advantages of oral dosing are driving further development of small molecule angiogenesis inhibitors.

The reports of the antiangiogenic activity of fumagillin and a semisynthetic analogue **3**, (TNP-470, AGM-1470), spurred efforts to determine its molecular target in vivo. In 1997, employing biotin or photoaffinity labeled conjugates of fumagillin and the closely related natural product ovalicin, two groups identified the molecular target of fumagillin as the enzyme methionine aminopeptidase type II (MetAP2), which cleaves the N-terminal methioninyl residue of newly synthesized proteins (Figure 1a).[3] Subsequent X-ray crystallographic[4] and biochemical studies[5] identified a covalent linkage of fumagillin and MetAP2 between His-231, located

*To whom correspondence should be addressed. Phone: 781-795-4272. Fax: 781-890-7015. E-mail: christopher.c.arico-muendel@gsk.com. (C.A.M.); Christopher.self@providpharma.com (C.S.); lily5719@yahoo.com (L.L.S.).

[a]Abbreviations: MetAP2, methionine aminopeptidase-2; VEGF, vascular endothelial growth factor; MTT, methylthiazolyldiphenyl-tetrazolium bromide; CNS, central nervous system; EH, epoxide hydrolase; HPLA, hydroxypropylmethacrylamide; PEG, polyethylene glycol; NMR, nuclear magnetic resonance; TFA, trifluoroacetic acid; HPLC, high performance liquid chromatography; DIEA, diisopropylethylamine; LRMS, low resolution mass spectrometry; HEPES, 4-(2-hydroxyethyl)-1-piperazineethanesulfonic acid; HUVEC, human vascular endothelial cell; BAEC, bovine aortic endothelial cell; ADME, absorption, distribution, metabolism, and excretion; $t_{1/2}$, elimination half-life; C_{max}, maximum concentration achieved; T_{max}, time of maximum concentration; AUC, area under curve; $F_{(oral)}$, oral bioavailability.

Published on Web 11/24/2009

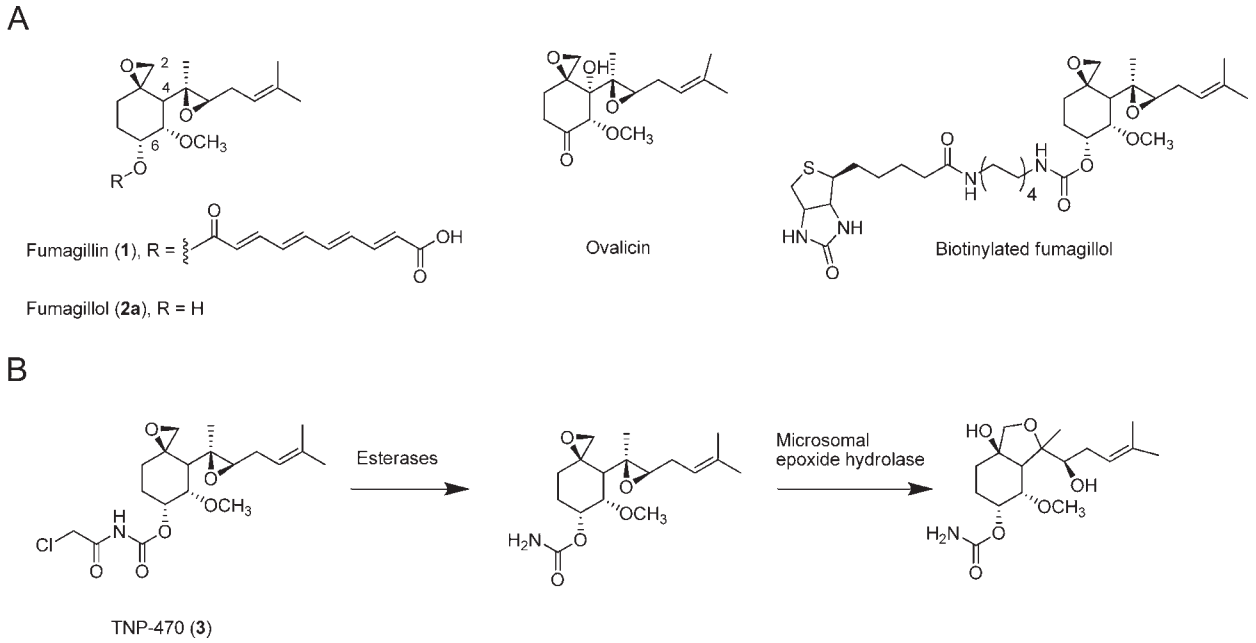

Figure 1. (A) Structures of fumagillin, fumagillol, ovalicin, and biotin-fumagillin conjugate.[3b] (B) Proposed mechanism for TNP-470 metabolism.[12]

in the enzyme active site, and C2 of the fumagillin spiroepoxide group. In particular, the crystal structure demonstrated that interaction of the C4 side chain, bearing the second, less reactive epoxide group, with the hydrophobic specificity pocket of the enzyme served to position the spiroepoxide precisely for attack by Nε2 of the histidine imidazole ring. In agreement with the previous data, the polyolefinic side chain of fumagillin extended out of the active site and was relatively unconstrained.

Identification of MetAP2 as a potential target for antiangiogenic therapy prompted widespread efforts to understand its mechanism of action, employing both chemical and biological approaches. The fumagillin analogue **3**, disclosed by Takeda, exhibited enhanced antiproliferative effects in vitro and demonstrated potent activity against a broad array of tumors in xenograft models.[6] The dose dependence of inhibition in HUVEC, in particular, was shown to be biphasic, with the first phase (GI_{50} = 37 pM) being cytostatic and fully reversible, whereas the high dose phase was cytotoxic and irreversible. In endothelial cells, MetAP2 inhibition was shown to affect amino terminal protein processing and activate the p53 pathway, leading to accumulation of the CDK inhibitor $p21^{WAF1/CIP1}$ and G1 cell cycle arrest.[7] The importance of MetAP-2 as the key regulator of endothelial cell proliferation was demonstrated by the equivalent and nonadditive effects of MetAP-2 functional downregulation either by siRNA or fumagillin and its analogues.[8] Recently, Liu's group correlated MetAP1/2 inhibition with regulation of c-Src and retardation of cell cycle progression.[9]

Several groups have employed fumagillin as starting points for MetAP-2 targeting therapeutics.[6] Among these, **3** progressed farthest, ultimately to phase 2 clinical studies, where it showed some benefits in both single and combination dosing for a number of cancers.[2,6] Efficacy of **3** has also been also demonstrated in rodent models of rheumatoid arthritis, another disease characterized by an angiogenic component.[10] However, the development of **3** has been hindered by poor pharmacokinetics, lack of oral bioavailability, and dose-limiting CNS side effects.[11] Studies by Sommadossi and co-workers revealed that **3** was rapidly hydrolyzed in plasma to an unsubstituted carbamate, which in turn was efficiently degraded by epoxide hydrolase (EH) (Figure 1b).[12] Caplostatin and lodamin,[13] comprising HPLA- and PEG-conjugates of **3**, respectively, addressed the PK liabilities and inhibited tumor formation in animals. In pursuing a small molecule strategy, we reasoned that replacement of the labile chloroacetyl group could suppress EH mediated degradation. Furthermore, the position of the C6 substituent away from the active site of the enzyme offered an opportunity to modulate the pharmacokinetic properties of the molecule without affecting its ability to inhibit MetAP2. We thus sought to incorporate functionality to minimize brain uptake and restrict circulation of the drug to the periphery. Here, we describe this design strategy and present SAR studies around C6 substituted fumagillin analogues in enzymatic and cell proliferation assays. The new compounds potently inhibit MetAP2 with SAR that can be interpreted in terms of interactions with the active site gatekeeper residues. Preliminary PK and safety data showed significant improvements relative to **3**, validating the design approach.

Results and Discussion

Several groups have described syntheses and biological activities of fumagillin analogues.[14] In designing novel fumagillin-based MetAP2 inhibitors that would improve upon the in vivo properties of **3**, we were guided by the following interpretations of the structural and biochemical data: (1) the cyclohexane spiroepoxide, or a reactive analogue, together with the C4 side chain, constituted a necessary and sufficient scaffold for potent inhibition, (2) the solvent exposed C6 side chain offered the best opportunity for modifications that would not compromise enzyme binding, and (3) the ADME liabilities of **3**, including both its rapid degradation by EH and its uptake into the CNS, could be remedied by replacement of the chloroacetyl group with a stable, more polar functionality. We reasoned that fumagillol, readily accessible from commercial fumagillin, represented a convenient source of the inhibitory core. The crystal structure of MetAP-2 containing a

bound fumagillin molecule reveals two hydrophobic side chains, Leu-328 and Leu-447, which serve as gatekeepers to the active site.[4] As a starting point for design, we chose carbamates of branched, hydrophobic amino acids that could interact with the leucine residues.[15] Linkage to the fumagillin core via a carbamate function, as opposed to an ester, was expected to impart chemical stability and allowed for elaboration of the amino acid carboxyl group as a variety of amides. Synthesis of the initial series was accomplished in a straightforward way by saponifying commercially available (+)-fumagillin to fumagillol, which was then activated as a *p*-nitrophenyl or *N*-hydroxysuccinimidyl carbonate ester and then derivatized with amines. The HOSu carbonate ester could be prepared on a multigram scale and purified by precipitation from isopropyl alcohol, allowing a diverse array of carbamates to be prepared (Scheme 1). Activities of these constructs against MetAP2 and in endothelial cell proliferation are summarized in Table 1.

Scheme 1. Synthesis of Fumagillol Derivatives[a]

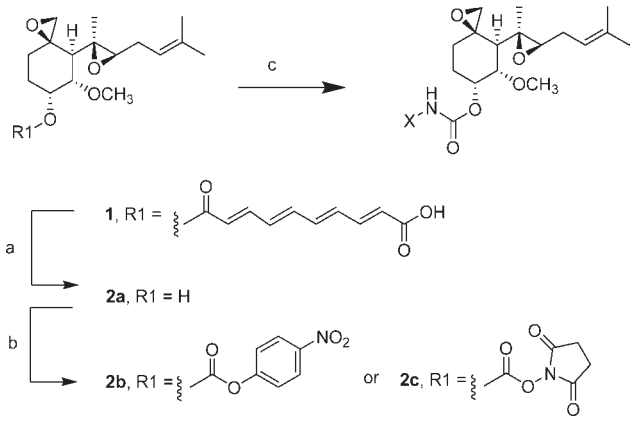

[a] Reagents: (a) NaOH, MeOH, H_2O, 0 °C → RT, 18 h; (b) *p*-nitrophenylchloroformate or DSC, TEA, CH_3CN, RT; (c) NH-X, DIEA, CH_3CN, RT, 18 h.

Methyl esters of both L- and D-valine (**4**, **5**) were found to potently inhibit proliferation in endothelial cells, as did structural homologues such as leucine (**6**) and phenylglycine (**7**). D-Valine amide (**8**) and alcohol (**9**) were also highly active. However, the D-valine free acid exhibited reduced activity in both the biochemical and cellular assay, as well as reduced chemical stability due to acid-mediated hydrolysis of the spiroexpoxide group (data not shown). Collectively, the simple amino acid based carbamates equaled or exceeded the activity of **3** in HUVEC growth inhibition.

In addition to antiproliferative activity, we compared the rate of MetAP2 inhibition by these compounds in a biochemical assay. MetAP-2 activity may be measured by quantitation of methionine release from peptidic substrates such as

Table 1. Inhibitory Activity of α-Amino Acid Analogues in MetAP2[a] and Cellular Growth Inhibition[b] Assays

Compound		MetAP2 (% activity)	HUVEC IC_{50} (nM)	BAEC IC_{50} (nM)
3	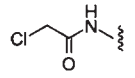	4.0	0.25	ND
4	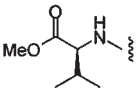	ND	0.018	0.017
5	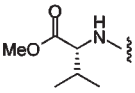	ND	0.040	0.048
6	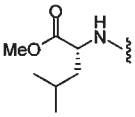	ND	0.038	0.118
7	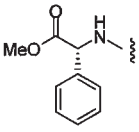	ND	0.036	0.035
8	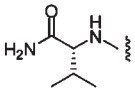	2.8	0.095	0.046
9	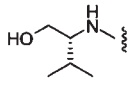	ND	ND	0.128

[a] Presented as percent activity remaining after 8 h treatment with compound. ND, not determined. [b] 50% inhibition in HUVEC and BAEC growth assays.

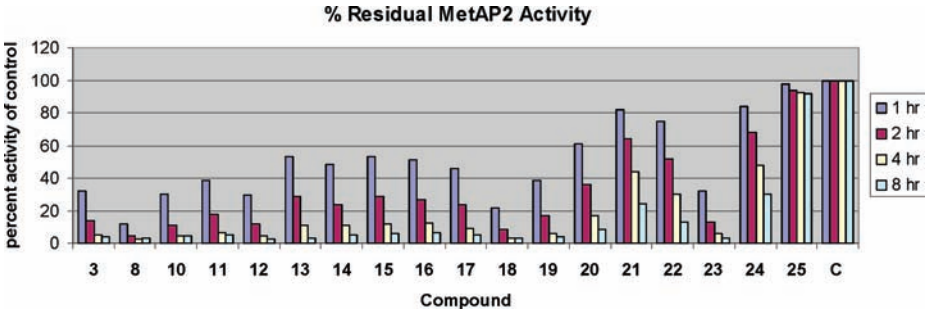

Figure 2. Time dependence of MetAP2 activity upon treatment with selected compounds. C: ethanol control.

Table 2. Inhibitory Activity of Charged Analogues in MetAP2[a] and Cellular Growth Inhibition[b] Assays

Compound		MetAP2 (% activity)	HUVEC IC_{50} (nM)
10	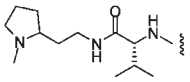	4.5	0.6
11	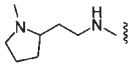	5.4	0.2
12	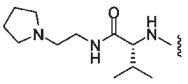	2.6	0.6
13	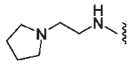	3.5	0.1
14	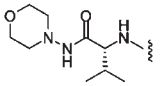	5.2	1.7
15	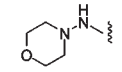	5.7	0.7
16	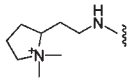	6.3	>100
17	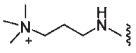	5.4	>100
18	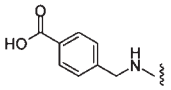	3.5	0.7
19	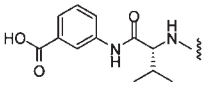	4.3	15
20	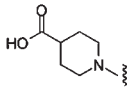	8.3	1.3

[a] Presented as percent activity remaining after 8 h treatment with compound. [b] 50% inhibition in HUVEC and BAEC growth assays.

Met-Gly-Met-Met.[16] However, this assay requires relatively high enzyme concentrations (> 20 nM), limiting its ability to identify highly potent inhibitors.[17] We found that while MetAP2 activity diminished toward zero in the presence of excess inhibitor, the rate of inhibition varied considerably (Figure 2). This behavior is consistent with irreversible (slow off-rate) inhibition superimposed on a range of on-rates.

Table 3. Inhibitory Activity of Dialkylated Amino Acid Analogues and Truncates in MetAP2[a] and Cellular Growth Inhibition[b] Assays

Compound		MetAP2 (% activity)	HUVEC IC_{50} (nM)
21	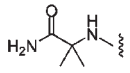	24	1.7
22	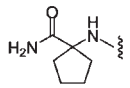	13	0.7
23		3	0.06
24		30	1.1

[a] Presented as percent activity remaining after 8 h treatment with compound. [b] 50% inhibition in HUVEC and BAEC growth assays.

Therefore, we employed residual enzyme activity in the presence of excess inhibitor as a surrogate for potency. This approach also allowed for comparisons with end-point-based determinations of MetAP-2 activity in vivo.[18]

The scope of the carbamate-based strategy was explored further by capping the C6 substituent with charged groups that might interact with exterior solvent. Analogues in which the D-valinamide moiety was extended with, or replaced by, aminoethylpyrrolidines (**10** and **12**, and **11** and **13**, respectively) showed nearly complete inhibition of MetAP-2 after 8 h, as well as subnanomolar inhibition of HUVEC proliferation (Figure 2, Table 2). Acyl hydrazines **14** and **15** also showed good activity in both assays. On the other hand, quaternary amine compounds **16** and **17**, while potent enzyme inhibitors, were less effective in the HUVEC assay, presumably because of poor cellular permeability, as were derivatives **18**, **19**, and **20**, in which the D-Val moiety was extended or replaced by carboxylate containing functionalities.

To examine further the scope of allowed hydrophobic linkers, we replaced the D-Val moiety with two dialkylamino acids, α,α-dimethyl- and cyclopentylglycine (**21** and **22**, respectively). In comparison with valine, both of these linkers resulted in a significant loss of inhibitory activity in both assays (Table 3). Further simplification of the structures yielded the isopropyl compound **23**, which was highly active, in contrast to the *t*-butyl compound **24**, which showed only 30% inhibition after 8 h, thus localizing the origins of this

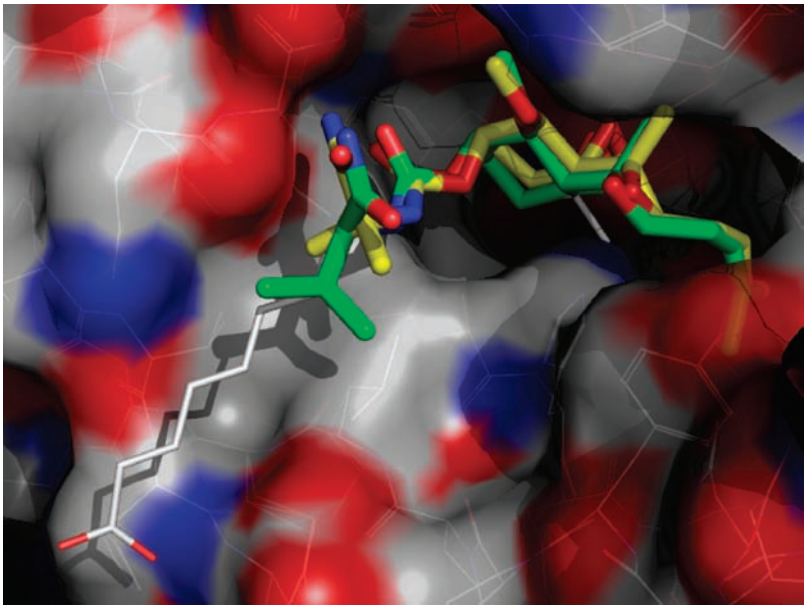

Figure 3. Structure of human MetAP2 (1BOA) in a complex with fumagillin (white), overlaid with docked structures of **8** (green) and **21** (yellow). Oxygen and nitrogen atoms are colored red and blue, respectively.

effect to the substitution of the α carbon. In the MetAP2 crystal structure, Leu-328 and -447 approach the polyolefinic ester of fumagillin at carbons 3 and 4; presumably, similar contacts with the carbamates are incompatible with tertiary substitution of the group closest to the fumagillol scaffold, whereas a broad variety of more distal substitutions are tolerated.[4] Binding models of several active molecules were generated to test this theory by constraining their fumagillol core to that of the crystal structure and minimizing the energy of the compound plus surrounding residues. In agreement with the hypothesis, the structure of **8** can be closely superimposed upon that of fumagillin, as shown in Figure 3. The D-chirality at the amino acid may also be inverted to L without noticeable alterations to the molecular geometry. However, the dimethyl substituted compound **21** undergoes noticeable conformational adjustments due to interactions with Asn327, suggesting that the α,α-dialkyl substitution destabilizes the bound form of the inhibitor.

The presence of reactive functionalities on fumagillin and the covalent basis for its mechanism of action have led to concerns about the viability of this compound class as a therapeutic due to potential off-target toxicities. However, probing cell lysates with immobilized fumagillin analogues has generally failed to identify alternative targets (data not shown). The issue may also be addressed by testing the inherent reactivity of the spiroepoxide core against MetAP2. We prepared 1-oxaspiro[2.5]octane, **25**, which showed only trace inhibition in the enzyme assay and did not inhibit HUVEC proliferation (Figure 4). Thus, the potency of fumagillin against MetAP2 results from a more complex network of noncovalent interactions rather than from a nonspecific alkylating capability. Taking an orthogonal approach, Liu's group recently reported two analogues of fumagillin, fumagalone and fumarranol, in which the reactive epoxide is replaced with retention of MetAP2 inhibition.[17] In fumagalone, the spiroepoxide function of fumagillin is replaced with a hydroxyaldehyde, and the C6 side chain with a ketone, converting the scaffold into a reversible inhibitor that retains its specificity for MetAP2 over MetAP1. In fumarranol, an intramolecular alkylation opens the epoxide into a hydroxymethyl group while bridging the cyclohexyl ring. Both examples highlight the contribution to binding of the C4 substituent that mimics the side chain of the methionine substrate.

Residual MetAP2 activity after 8h treatment: 92%

HUVEC IC_{50}: >100 nM

25

Figure 4. Structure and activity of compound **25**.

Following in vitro screening, a subset of the more potent analogues were subjected to initial PK and toxicology studies. In particular, we found that rats treated daily for 14 consecutive days with **8** at 6 and 60 mg/kg (iv) demonstrated a significantly improved CNS toxicity profile over **3**, measured by incidence of seizures. While several animals treated with 6 mg/kg and all animals treated with 60 mg/kg **3** developed seizures, none of the animals treated with **8** at either dose developed seizures or showed other clinical signs of toxicity.[18] This outcome supports the premise that the in vivo liabilities of **3** could be addressed by reengineering a component of the molecule not required for inhibition. In addition, **8** was further tested in a cassette PK study along with **10**, **11**, and **12** (Table 4). All four compounds show a significant increase in $t_{1/2}$ relative to **3**, whose reported half-life in human studies was as short as 2 min.[11b,d,f] The oral bioavailabilities of all four compounds based on parent molecule plasma concentration were found to be modest, although they could be somewhat improved by the addition of charged functionality. Taken together, the results suggest that the carbamate-based analogues either fail to enter the CNS due to their higher polarity, or resist modification to brain penetrant species that cause CNS toxicity. Additional studies of **8** have led to the discovery of six active cytochrome P_{450}-derived metabolites that supplement the efficacy of the parent molecule in vivo. A detailed characterization of these species, including identification, chemical synthesis, and MetAP2 inhibitory activity, has been performed and will be reported separately.

Table 4. Pharmacokinetic Data for Selected Compounds in Rats

	route of administration	dose (mg/kg)	T_{max} (min)	C_{max} (ng/mL)	AUC (min·ng/mL)	$t_{1/2}$[a] (min)	clearance (mL/min)	$F_{(oral)}$ (%)
8	iv	5	0	584	8540	13/103	283	
8	oral	10	15	35	1540	20/178	5760	9.0
10	iv	5	0	456	22400	54	220	
10	oral	10	120	27	7310	196	946	16.3
11	iv	5	0	246	6660	27/120	742	
11	oral	10	15	15	2440	168	3180	18.3
12	iv	5	0	2640	38900	16/67	128	
12	oral	10	60	31	8150	233	772	10.5

[a] Where applicable, shown as both initial and terminal half-lives.

Conclusion

We have reported a novel series of fumagillin analogues containing carbamate-linked amines at C-6 of the oxirane core. These analogues were designed to preserve the high affinity of fumagillin for MetAP2 while stabilizing the scaffold toward metabolism and limiting its CNS uptake. The compounds show rapid inactivation of MetAP2 in a biochemical assay, as well as potent antiproliferative activity against HUVEC. As predicted by the fumagillin-MetAP2 crystal structure, our data confirm that a wide variety of substituents are tolerated at the C6 side chain; however, we demonstrate that sterically demanding functions proximate to the cyclohexane ring are not accommodated, and this result may be explained by a docking study. The first generation lead compound, **8** (PPI-2458), was found to potently inhibit MetAP2 enzymatic activity and endothelial cell proliferation. Notably, **8** also shows efficacy in animal models for melanoma and non-Hodgkin's lymphoma[19] as well as for rheumatoid arthritis, following oral administration.[18,20] These outcomes, together with the lack of CNS toxicity, suggest that the major pharmacokinetic and toxicological liabilities of **3** have been remedied. Having demonstrated efficacy in multiple animal models, **8** was advanced into proof-of-concept studies in man. The collective in vivo findings for **8** will help to establish the validity of MetAP2 inhibition as a novel approach for anti-angiogenic therapy.

Experimental Section

General. Commercially available reagents and solvents were used as purchased without further purification. Fumagillin dicyclohexylamine salt was obtained from CEVA. Compound **3** was prepared according to the published procedure.[6a] Analytical LC-MS was performed on a HP-1100 system interfaced with a Finnegan LCQ Advantage electrospray mass spectrometer, using Phenomenex Luna C8(2) 3 μm columns with acetonitrile/0.1% aqueous TFA elution. Preparative HPLC was performed on a Gilson system with a Phenomenex Luna C8(2), 5 μm, 100 mm × 21.2 mm column at a flow rate of 24 mL/min and detection at 214 nm. To avoid acid catalyzed degradation, preparative LC was performed without TFA in the eluting solvents. Thin layer chromatography was performed on 250 μm EM Science silica gel 60 plates using UV_{254} or iodine visualization. NMR spectra were obtained on a Varian MercuryPlus 400 MHz spectrometer referenced to TMS at 0.0 ppm. In general, final compound purities were 95% or greater as determined by HPLC-MS.

(3*R*,4*S*,5*S*,6*R*)-5-Methoxy-4-((2*R*,3*R*)-2-methyl-3-(3-methylbut-2-enyl)oxiran-2-yl)-1-oxaspiro[2.5]octan-6-ol, (fumagillol, 2a). Fumagillin dicyclohexylamine salt (30 g, 47.0 mmol) was suspended in 300 mL of 1:1 methanol:water and treated with 10.7 mL of 35% NaOH solution (94 mmol). The dark-brown mixture was stirred in an ice bath for 2 h, then warmed to room temperature and treated with another equivalent of NaOH solution. The mixture was stirred until starting material was not detected by TLC (~4 h); the methanol was evaporated and the residue extracted into ethyl acetate. The mixture was then extracted with 5% citric acid, brine, bicarbonate, and brine again, then dried with $MgSO_4$ and concentrated in vacuo. The crude product was further purified by treatment with activated charcoal in acetonitrile and filtration through a celite pad. Concentration yielded a colorless oil, 10.36 g (78%). ^{1}H NMR (CD_3OD): δ 5.23 (t, 1H), 4.36 (m, 1H), 3.54 (dd, 1H), 3.42 (s, 3H), 2.92 (d, 1H), 2.64 (t, 1H), 2.52 (d, 1H), 2.2−2.4 (m, 2H), 2.15 (dd, 1H), 1.94 (d, 1H,), 1.7−1.9 (m, 2H), 1.75 (d, 3H), 1.67 (d, 3H), 1.19 (s, 3H), 0.96 (m, 1H).

2,5-Dioxopyrrolidin-1-yl (3*R*,4*S*,5*S*,6*R*)-5-methoxy-4-((2*R*,3*R*)-2-methyl-3-(3-methylbut-2-enyl)oxiran-2-yl)-1-oxaspiro[2.5]octan-6-yl Carbonate (Fumagillol *N*-Hydroxysuccinimidyl Carbonate Ester, 2c). Fumagillol (10.36 g, 36.68 mmol) was dissolved in 25 mL of acetonitrile and treated with triethylamine (15.34 mL, 110 mmol), and *N*,*N*′-disuccinimidyl carbonate (18.80 g, 73.37 mmol). The tan slurry was stirred at room temperature under nitrogen for 4 h, then treated with celite, activated charcoal, and anhydrous sodium sulfate and filtered through a celite pad. The solution was concentrated, taken up in ethyl acetate, and washed with bicarbonate solution, brine, 5% citric acid, and brine, then dried over $MgSO_4$ and concentrated to an amber oil. The residue was precipitated from cold isopropyl alcohol to yield a white solid, 8.33 g (54%). ^{1}H NMR (CD_3OD): δ 5.54 (m, 1H), 5.23 (t, 1H), 3.78 (dd, 1H), 3.43 (s, 3H), 2.98 (d, 1H), 2.82 (s, 4H), 2.69 (t, 1H), 2.60 (d, 1H), 2.32 (m, 1H), 2.06−2.24 (m, 2H), 1.96 (m, 1H), 1.90 (d, 1H), 1.75 (d, 3H), 1.67 (d, 3H), 1.20 (s, 3H), 1.16 (m, 1H).

Substitution of 2b with Amines (General Procedure A). To a mixture of carbonic acid-(3*R*, 4*S*, 5*S*, 6*R*)-5-methoxy-4-[(2*R*, 3*R*)-2-methyl-3-(3-methyl-but-2-enyl)-oxiranyl]-1-oxaspiro[2.5]-oct-6-yl ester 4-nitro-phenyl ester (**2b**)[14] (0.47 mmol) and amine (2.35 mmol) in EtOH (9 mL) was added dropwise, diisopropyl ethyl amine (2.35 mmol). After 3−18 h, the ethanol was removed in vacuo and the crude material was dissolved into EtOAc (10 mL) and washed with H_2O (2 × 5 mL), and then brine (5 mL). The organic phase was dried over Na_2SO_4 and the solvent removed in vacuo. Purification via flash chromatography (2−5% MeOH/CH_2Cl_2) afforded product.

Substitution of 2c with Amines (General Procedure B). 2c (2 mmol) was stirred in acetonitrile with amine salt (4.0 mmol) in an ice bath. DIEA (4.0 mmol) was added, and the solution stirred under nitrogen overnight. Extractive workup and purification was performed as in procedure A. For polar products, purification was performed by preparative HPLC.

Synthesis of Amino Amides (General Procedure C). Boc-amino acid (2.0 mmol) was dissolved in 3 mL THF, and stirred in an ice bath under nitrogen. *N*-Methyl morpholine (220 μL, 2.0 mmol) and isobutylchloroformate (260 μL, 2.0 mmol) were added, and the mixture was stirred for 5 min. A white precipitate was removed by filtration, and the filtrate was treated with amine. The solution was stirred at 0 °C for 20 min and then warmed to room temperature and stirred 20 min more. The solution was concentrated in vacuo and reduced to a solid under high vacuum. It was then treated with 20 mL of 4 M HCl in dioxane for an hour at room temperature. Concentration and trituration with ether yielded a white powder of acceptable purity for acylation with **2c**. Alternatively, **2c** was used to *N*-acylate the free amino acid, and the product was then converted to a substituted amide as a separate step.

(*S*)-Methyl 2-(((3*R*,4*S*,5*S*,6*R*)-5-Methoxy-4-((2*R*,3*R*)-2-methyl-3-(3-methylbut-2-enyl)oxiran-2-yl)-1-oxaspiro[2.5]octan-6-yloxy)-carbonylamino)-3-methylbutanoate (4). General procedure A was followed using **2b** (31 mg, 0.07 mmol), L-valine methyl ester hydrochloride (58 mg, 0.35 mmol), and DIEA (60 μL, 0.35 mmol) in EtOH (2 mL). Purification via flash chromatography (1% MeOH/CH_2Cl_2) afforded the product as a clear oil

(10 mg, 0.02 mmol, 33% yield); R_f = 0.60 (20% EtOAc/CH_2Cl_2). LRMS (m/z) $[M + 1]^+$ 440.3 (calculated for $C_{23}H_{38}NO_7$, 440.3). ^{1}H NMR (CD_3OD; conformers due to slow carbamate *cis*−*trans* interconversion indicated as a second chemical shift): δ 5.47, 5.04 (s, 1H), 5.24 (t, 1H), 4.07, 4.00 (d, 1H), 3.71 (s, 3H), 3.68 (dd, 1H), 3.41 (s, 3H), 2.96 (d, 1H), 2.65 (t, 1H), 2.56 (d, 1H), 2.32 (m, 1H), 2.23 (m, 1H), 2.11 (m, 2H), 2.00 (d, 1H), 1.95 (m, 1H), 1.82 (m, 1H), 1.76 (s, 3H), 1.67 (s, 3H), 1.20 (s, 3H), 1.06 (m, 1H), 1.00, 0.94(m, 6H).

(*R*)-Methyl 2-(((3*R*,4*S*,5*S*,6*R*)-5-Methoxy-4-((2*R*,3*R*)-2-methyl-3-(3-methylbut-2-enyl)oxiran-2-yl)-1-oxaspiro[2.5]octan-6-yloxy)carbonylamino)-3-methylbutanoate (5). General procedure A was followed using **2b** (41 mg, 0.09 mmol) and D-valine methyl ester hydrochloride (77 mg, 0.45 mmol) and DIEA (80 μL, 0.45 mmol) in EtOH (2 mL). Purification via flash chromatography (1% MeOH/CH_2Cl_2) afforded the product as a clear oil (18 mg, 0.04 mmol, 45% yield); R_f = 0.39 (20% EtOAc/CH_2Cl_2. LRMS (m/z) $[M + 1]^+$ 440.3 (calculated for $C_{23}H_{38}NO_7$, 440.3). ^{1}H NMR (CD_3OD): δ 7.24 (d, 1H), 5.42 (m, 1H), 5.24 (m, 1H), 4.07 (m, 1H), 3.71 (s, 3H), 3.67 (dd, 1H), 3.38 (s, 3H), 2.96 (d, 1H), 2.64 (t, 1H), 2.56 (d, 1H), 2.30 (m, 1H), 2.21 (m, 1H). 2.12 (m, 2H), 2.01 (d, 1H), 1.97 (m, 1H), 1.82 (m, 1H), 1.75 (s, 3H), 1.67 (s, 3H), 1.19 (s, 3H), 1.04 (m, 1H), 0.95 (m, 6H).

(*R*)-Methyl 2-(((3*R*,4*S*,5*S*,6*R*)-5-Methoxy-4-((2*R*,3*R*)-2-methyl-3-(3-methylbut-2-enyl)oxiran-2-yl)-1-oxaspiro[2.5]octan-6-yloxy)carbonylamino)-4-methylpentanoate (6). General procedure A was followed using **2b** (23 mg, 0.05 mmol), D-leucine methyl ester hydrochloride (47 mg, 0.25 mmol), and DIEA (45 μL, 0.25 mmol) in EtOH (2 mL). Purification via flash chromatography (1% MeOH/CH_2Cl_2) afforded the product as a clear oil (19 mg, 0.04 mmol, 83% yield); R_f = 0.22 (15% EtOAc/CH_2Cl_2). LRMS (m/z) $[M + 1]^+$ 454.3 (calculated for $C_{24}H_{40}NO_7$, 454.3). ^{1}H NMR (CD_3OD): δ 5.43 (m, 1H), 5.23 (t, 1H), 4.22 (m, 1H), 3.70 (s, 3H), 3.67 (dd, 1H), 3.40 (s, 3H), 2.96 (d, 1H), 2.63 (t, 1H), 2.56 (d, 1H), 2.32 (m, 1H), 2.23 (m, 1H), 2.15 (m, 1H), 1.98 (d, 1H), 1.93 (m, 1H), 1.82 (m, 1H), 1.76 (s, 3H), 1.72 (m, 1H), 1.67 (s, 3H), 1.57 (m, 2H), 1.19 (s, 3H), 1.06 (s, 1H), 0.94 (m, 6H).

(*R*)-Methyl 2-(((3*R*,4*S*,5*S*,6*R*)-5-Methoxy-4-((2*R*,3*R*)-2-methyl-3-(3-methylbut-2-enyl)oxiran-2-yl)-1-oxaspiro[2.5]octan-6-yloxy)carbonylamino)-2-phenylacetate (7). General procedure A was followed using **2b** (37 mg, 0.08 mmol), D-phenyl glycine methyl ester hydrochloride (83 mg, 0.40 mmol), and DIEA (72 μL, 0.40 mmol) in EtOH (2 mL). Purification via flash chromatography (1% MeOH/CH_2Cl_2) afforded the product as a clear oil (32 mg, 0.07 mmol, 82% yield); R_f = 0.41 (2% MeOH/CH_2Cl_2). LRMS (m/z) $[M + 1]^+$ 474.3 (calculated for $C_{26}H_{36}NO_7$, 474.3). ^{1}H NMR (CD_3OD; conformers due to slow carbamate *cis*−*trans* interconversion indicated as a second chemical shift): δ 7.36 (m, 5H), 5.44, 5.37 (m, 1H), 5.28 (s, 1H), 5.22 (t, 1H), 3.70 (s, 3H), 3.66 (dd, 1H), 3.36 (s, 3H), 2.96 (d, 1H), 2.62 (t, 1H), 2.56 (d, 1H), 2.31 (m, 1H), 2.20 (m, 2H), 1.98 (d, 1H), 1.83 (m, 1H), 1.70 (s, 3H), 1.70 (m, 1H), 1.66 (s, 3H), 1.18 (s, 3H), 1.06 (m, 1H).

(3*R*,4*S*,5*S*,6*R*)-5-Methoxy-4-((2*R*,3*R*)-2-methyl-3-(3-methylbut-2-enyl)oxiran-2-yl)-1-oxaspiro[2.5]octan-6-yl (*R*)-1-Amino-3-methyl-1-oxobutan-2-ylcarbamate (8). General procedure A was followed using **2b** (55 mg, 0.12 mmol), D-valine amide hydrochloride (93 mg, 0.62 mmol), and DIEA (110 μL, 0.62 mmol) in EtOH (2 mL). Purification via flash chromatography (2% MeOH/CH_2Cl_2) afforded the product as a clear oil (42 mg, 0.10 mmol, 80% yield); R_f = 0.19 (2% MeOH/CH_2Cl_2). LRMS (m/z) $[M + 1]^+$ 425.5 (calculated for $C_{22}H_{37}N_2O_6$, 425.5). ^{1}H NMR (CD_3OD; conformers due to slow carbamate *cis*−*trans* interconversion indicated as a second chemical shift): δ 5.43 (m, 1H), 5.24 (t, 1H), 3.94 (d, 1H), 3.67 (dd, 1H), 3.40 (s, 3H), 2.96 (d, 1H), 2.64 (t, 1H), 2.56 (d, 1H), 2.31 (m, 1H), 2.22 (m, 1H), 2.14 (m, 1H), 1.97 (d, 1H), 1.96 (m, 1H), 1.80 (m, 1H), 1.75 (s, 3H), 1.67 (s, 3H), 1.19 (s, 3H), 1.04 (m, 1H), 0.99, 0.96 (m, 6H).

(3*R*,4*S*,5*S*,6*R*)-5-Methoxy-4-((2*R*,3*R*)-2-methyl-3-(3-methylbut-2-enyl)oxiran-2-yl)-1-oxaspiro[2.5]octan-6-yl (*R*)-1-Hydroxy-3-methylbutan-2-ylcarbamate (9). General procedure A was followed using **2b** (290 mg, 0.65 mmol), D-valinol (337 mg, 3.25 mmol), and DIEA (560 μL, 3.25 mmol) in EtOH (5 mL). Purification via flash chromatography (2% MeOH/CH_2Cl_2) afforded the product as a clear oil (200 mg, 0.49 mmol, 75% yield); R_f = 0.26 (2% MeOH/CH_2Cl_2). LRMS (m/z) $[M + 1]^+$ 412.5 (calculated for $C_{22}H_{38}NO_6$, 412.5). ^{1}H NMR (CD_3OD): δ 5.42 (m, 1H), 5.23 (t, 1H), 3.67 (dd, 1H), 3.59 (m, 1H), 3.52 (m, 1H), 3.40 (m, 1H), 3.40 (s, 3H), 2.96 (d, 1H), 2.63 (t, 1H), 2.56 (d, 1H), 2.31 (m, 1H), 2.23 (m, 1H), 2.12 (m, 1H), 1.99 (d, 1H), 1.98 (m, 1H), 1.84 (m, 2H), 1.75 (s, 3H), 1.67 (s, 3H), 1.20 (s, 3H), 1.05 (m, 1H), 0.94 (m, 6H).

(3*R*,4*S*,5*S*,6*R*)-5-Methoxy-4-((2*R*,3*R*)-2-methyl-3-(3-methylbut-2-enyl)oxiran-2-yl)-1-oxaspiro[2.5]octan-6-yl (2*R*)-3-Methyl-1-(2-(1-methylpyrrolidin-2-yl)ethylamino)-1-oxobutan-2-ylcarbamate (10). General procedure C was followed. LRMS (m/z) $[M + 1]^+$ 536.4 (calculated for $C_{29}H_{49}N_3O_6$, 536.4). ^{1}H NMR (CD_3OD): δ 5.43 (m, 1H), 5.24 (t, 1H), 3.84 (d, 1H), 3.67 (dd, 1H), 3.41 (s, 3H), 3.26 (m, 2H), 3.04 (m, 1H), 2.96 (d, 1H), 2.65 (t, 1H), 2.56 (d, 1H), 2.31 (m, 3H), 2.2 (m, 4H), 2.0 (m, 5H), 1.8 (m, 4H), 1.76 (s, 3H), 1.68 (s, 3H), 1.5 (m, 1H), 1.4 (m, 1H), 1.20 (s, 3H), 1.04 (m, 1H), 0.96 (d, 6H).

(3*R*,4*S*,5*S*,6*R*)-5-Methoxy-4-((2*R*,3*R*)-2-methyl-3-(3-methylbut-2-enyl)oxiran-2-yl)-1-oxaspiro[2.5]octan-6-yl 2-(1-Methylpyrrolidin-2-yl)ethylcarbamate (11). General procedure B was followed. LRMS (m/z) $[M + 1]^+$ 437.3 (calculated for $C_{24}H_{40}N_2O_5$, 437.3). ^{1}H NMR (CD_3OD): δ 5.44 (m, 1H), 5.24 (t, 1H), 3.66 (dd, 1H), 3.42 (s, 3H), 3.14 (m, 2H), 3.07 (m, 1H), 2.96 (d, 1H), 2.61 (t, 1H), 2.34 (d, 1H), 2.35 (s, 3H), 2.30 (m, 1H), 2.23 (m, 3H), 2.10 (m, 2H), 1.94 (m, 3H), 1.92 (m, 3H), 1.76 (s, 3H), 1.67 (s, 3H), 1.49 (m, 1H), 1.41 (m, 1H), 1.20 (s, 3H), 1.05 (m, 1H).

(3*R*,4*S*,5*S*,6*R*)-5-Methoxy-4-((2*R*,3*R*)-2-methyl-3-(3-methylbut-2-enyl)oxiran-2-yl)-1-oxaspiro[2.5]octan-6-yl (*R*)-3-Methyl-1-oxo-1-(2-(pyrrolidin-1-yl)ethylamino)butan-2-ylcarbamate (12). General procedure C was followed. LRMS (m/z) $[M + 1]^+$ 522.6 (calculated for $C_{28}H_{47}N_3O_6$, 522.3). ^{1}H NMR (CD_3OD): δ 5.43 (s, 1H), 5.24 (t, 1H), 3.84 (d, 1H), 3.68 (dd, 1H), 3.53 (m, 1H), 3.40 (m, 1H), 3.40 (s, 3H), 3.03 (m, 6 H), 2.96 (d, 1H), 2.64 (t, 1H), 2.56 (d, 1H), 2.31 (m, 1H), 2.24 (m, 1H), 2.15 (dt, 1H), 2.08 (d, 1H), 2.06 (d, 1H), 1.96 (m, 5H), 1.84 (m, 1H), 1.76 (s, 3H), 1.67 (s, 3H), 1.19 (s, 3H), 1.08 (m, 1H), 0.97 (d, 6H).

(3*R*,4*S*,5*S*,6*R*)-5-Methoxy-4-((2*R*,3*R*)-2-methyl-3-(3-methylbut-2-enyl)oxiran-2-yl)-1-oxaspiro[2.5]octan-6-yl 2-(Pyrrolidin-1-yl)ethylcarbamate (13). General procedure B was followed. LRMS (m/z) $[M + 1]^+$ 423.3 (calculated for $C_{23}H_{38}N_2O_5$, 423.3). ^{1}H NMR (CD_3OD): δ 5.45 (m, 1H), 5.24 (m, 1H), 3.66 (dd, 1H), 3.42 (s, 3H), 3.26 (m, 2H), 2.96 (d, 1 H), 2.60 (m, 7 H), 2.56 (d, 1H), 2.31 (m, 1H), 2.23 (m, 1H), 2.10 (m, 1H), 1.94 (m, 2H), 1.81 (m, 5 H), 1.76 (s, 3H), 1.67 (s, 3H), 1.20 (s, 3H), 1.05 (m, 1H).

(3*R*,4*S*,5*S*,6*R*)-5-Methoxy-4-((2*R*,3*R*)-2-methyl-3-(3-methylbut-2-enyl)oxiran-2-yl)-1-oxaspiro[2.5]octan-6-yl (*R*)-3-Methyl-1-(morpholinoamino)-1-oxobutan-2-ylcarbamate (14). General procedure C was followed. LRMS (m/z) $[M + 1]^+$ 510.5 (calculated for $C_{26}H_{43}N_3O_7$, 510.3). ^{1}H NMR (CD_3OD): δ 5.42 (m, 1H), 5.24 (m, 1H), 3.74 (m, 4H), 3.66 (m, 1H), 3.40 (s, 3H), 3.30 (m, 1H), 2.96 (d, 1H), 2.78 (t, 4H), 2.64 (t, 1H), 2.56 (d, 1H), 2.30 (m, 1H), 2.23 (m, 1H), 2.13 (m, 1H), 1.99 (m, 2H), 1.92 (m, 1H), 1.80 (m, 1H), 1.75 (s, 3H), 1.67 (s, 3H), 1.19 (s, 3H), 1.03 (m, 1H), 0.96 (m, 6H).

(3*R*,4*S*,5*S*,6*R*)-5-Methoxy-4-((2*R*,3*R*)-2-methyl-3-(3-methylbut-2-enyl)oxiran-2-yl)-1-oxaspiro[2.5]octan-6-yl Morpholinocarbamate (15). General procedure B was followed. LRMS (m/z) $[M + 1]^+$ 411.1 (calculated for $C_{21}H_{34}N_2O_6$, 411.2). ^{1}H NMR (CD_3OD) δ 5.50 (s, 1H), 5.23 (t, 1H), 3.73 (t, 4H), 3.67 (dd, 1H), 3.42 (s, 3H), 2.96 (1H), 2.77 (s, 4H), 2.62 (t, 1H), 2.57 (d, 1H), 2.31 (m, 1H), 2.24 (m, 1H), 2.09 (m, 1H), 1.92 (m, 2H), 1.84 (m, 1H), 1.75 (s, 3H), 1.67 (s, 3H), 1.19 (s, 3H), 1.06 (m, 1H).

2-(2-(((3*R*,4*S*,5*S*,6*R*)-5-Methoxy-4-((2*R*,3*R*)-2-methyl-3-(3-methylbut-2-enyl)oxiran-2-yl)-1-oxaspiro[2.5]octan-6-yloxy)-carbonylamino)ethyl)-1,1-dimethylpyrrolidinium Iodide (16). To a solution of **11** (52 mg, 0.119 mmol) in toluene (0.3 mL) was added iodomethane (0.89 mL, 14.4 mmol), and the mixture was stirred overnight. The resulting precipitate was washed with ether and purified by recrystallization from methanol/ether. LRMS (*m*/*z*) $[M]^+$ 451.4 (calculated for $C_{25}H_{43}N_2O_5^+$, 451.3). Elemental analysis: C, 51.81; H, 7.46; I, 21.96; N, 4.65 (calculated for $C_{25}H_{43}IN_2O_5$: C, 51.90; H, 7.49; I, 21.94; N, 4.84; O, 13.83).

3-(((3*R*,4*S*,5*S*,6*R*)-5-Methoxy-4-((2*R*,3*R*)-2-methyl-3-(3-methylbut-2-enyl)oxiran-2-yl)-1-oxaspiro[2.5]octan-6-yloxy)carbonylamino)-*N*,*N*,*N*-trimethylpropan-1-aminium Iodide (17). The chemistry was conducted as for **16**, starting with the corresponding dimethylamino compound, and using 40 equiv of iodomethane. LRMS (*m*/*z*) $[M]^+$ 425.3 (calculated for $C_{23}H_{41}N_2O_5^+$, 425.3); Elemental analysis: C, 50.13; H, 7.42; I, 22.80; N, 4.94 (calculated for $C_{23}H_{41}IN_2O_5$: C, 50.00; H, 7.48; I, 22.97; N, 5.07; O, 14.48).

4-((((3*R*,4*S*,5*S*,6*R*)-5-Methoxy-4-((2*R*,3*R*)-2-methyl-3-(3-methylbut-2-enyl)oxiran-2-yl)-1-oxaspiro[2.5]octan-6-yloxy)carbonylamino)methyl)benzoic Acid (18). General procedure B was followed. LRMS (*m*/*z*) $[M + 1]^+$ 460.1 (calculated for $C_{25}H_{33}NO_7$, 460.2). Elemental analysis: C, 65.52; H, 7.69; N, 3.88 (calculated for $C_{25}H_{33}NO_7$: C, 65.34; H, 7.24; N, 3.05; O, 24.37). ^{1}H NMR (CD_3OD): δ 8.01 (s, 2H), 7.35 (s, 2H), 5.48 (s,1H), 5.23 (t, 1H), 4.34 (m, 2H), 3.68 (d, 1H), 3.43 (s, 3H), 2.96 (d, 1H), 2.62 (t, 1H), 2.55 (d, 1H), 2.32 (m, 1H), 2.17 (m, 1H), 2.12 (m, 1H), 1.98 (m, 2H), 1.84 (m, 1H), 1.75 (s, 3H), 1.66 (s, 3H), 1.19 (s, 3H), 1.06 (m, 1H).

3-((*R*)-2-(((3*R*,4*S*,5*S*,6*R*)-5-Methoxy-4-((2*R*,3*R*)-2-methyl-3-(3-methylbut-2-enyl)oxiran-2-yl)-1-oxaspiro[2.5]octan-6-yloxy)-carbonylamino)-3-methylbutanamido)benzoic Acid (19). General procedure C was followed. LRMS (*m*/*z*) $[M + 1]^+$ 545.1 (calculated for $C_{29}H_{40}N_2O_8$, 545.3). Elemental analysis: C, 63.71; H, 7.28; N, 5.03 (calculated for $C_{29}H_{40}N_2O_8$: C, 63.95; H, 7.40; N, 5.14; O, 23.50). ^{1}H NMR (CD_3OD): δ 7.93 (s, 1H), 7.83 (d, 1H), 7.70 (d, 1H), 7.32 (t, 1H), 5.45 (s, 1H), 5.24 (t, 1H), 4.07 (d, 1H), 3.68 (d, 1H), 3.42 (s, 1H), 2.96 (d, 1H), 2.66 (t, 1H), 2. 56 (d, 1H), 2.31 (m, 1 H), 2.17 (m, 3H), 2.02 (d, 1H), 1.98 (m, 1H), 1.80 (m, 1H), 1.76 (s, 3H), 1.67 (s, 3H), 1.20 (s, 3 H), 1.02 (m, 7H).

1-(((3*R*,4*S*,5*S*,6*R*)-5-Methoxy-4-((2*R*,3*R*)-2-methyl-3-(3-methylbut-2-enyl)oxiran-2-yl)-1-oxaspiro[2.5]octan-6-yloxy)carbonyl)-piperidine-4-carboxylic Acid (20). General procedure B was followed. LRMS (*m*/*z*) $[M + 1]^+$ 438.2 (calculated for $C_{23}H_{35}NO_7$, 438.2). Elemental analysis: C, 62.94; H, 7.97; N, 3.15 (calculated for $C_{23}H_{35}NO_7$: C, 63.14; H, 8.06; N, 3.20; O, 25.60). ^{1}H NMR (CD_3OD): δ 5.48 (s, 1H), 5.24 (t, 1H), 4.06 (d, 2H), 3.76 (dd, 1H), 3.41 (s, 3H), 2.98 (d, 1H), 2.90 (m, 2H), 2.68 (t, 1H), 2.56 (d, 1H), 2.30 (m, 2H), 2.22 (m, 1H), 2.09 (m, 1H), 1.90 (m, 5H), 1.75 (s, 3H), 1.67 (s, 3H), 1.59 (m, 2H), 1.19 (s, 3H), 1.08 (d, 1H).

(3*R*,4*S*,5*S*,6*R*)-5-Methoxy-4-((2*R*,3*R*)-2-methyl-3-(3-methylbut-2-enyl)oxiran-2-yl)-1-oxaspiro[2.5]octan-6-yl 1-Amino-2-methyl-1-oxopropan-2-ylcarbamate (21). General procedure B was followed. LRMS (*m*/*z*) $[M + 1]^+$ 411.6 (calculated for $C_{21}H_{34}N_2O_6$, 411.2). ^{1}H NMR (CD_3OD): δ 5.45 (s, 1H), 5.24 (t, 1H), 3.65 (d, 1H), 3.40 (s, 3H), 2.96 (d, 1H), 2.64 (m, 1H), 2.56 (d, 1H), 2.32 (m, 1H), 2.23 (m, 1H), 2.15 (dt, 1H), 1.98 (d, 1H), 1.88 (m, 1H), 1.84 (m, 1H), 1.76 (s, 3H), 1.68 (s, 3H), 1.46 (s, 3H), 1.42 (s, 3H), 1.18 (s, 3H), 1.04 (1H).

(3*R*,4*S*,5*S*,6*R*)-5-Methoxy-4-((2*R*,3*R*)-2-methyl-3-(3-methylbut-2-enyl)oxiran-2-yl)-1-oxaspiro[2.5]octan-6-yl 1-Carbamoylcyclopentylcarbamate (22). General procedure B was followed. LRMS (*m*/*z*) $[M + 1]^+$ 437.5 (calculated for $C_{23}H_{36}N_2O_6$, 437.3). ^{1}H NMR (CD_3OD): δ 5.45 (s, 1H), 5.24 (t, 1H), 3.66 (dd, 1H), 3.40 (s, 3H), 2.96 (d, 1H), 2.63 (t, 1H), 2.56 (d, 1H), 2.31 (m, 2H), 2.18 (m, 2H), 1.99 (m, 3H), 1.87 (m, 3H), 1.76 (m, 4H), 1.76 (s, 3H), 1.68 (s, 3H), 1.18 (s, 3H), 1.04 (d, 1H).

(3*R*,4*S*,5*S*,6*R*)-5-Methoxy-4-((2*R*,3*R*)-2-methyl-3-(3-methylbut-2-enyl)oxiran-2-yl)-1-oxaspiro[2.5]octan-6-yl Isopropylcarbamate (23). General procedure B was followed. LRMS (*m*/*z*) $[M + 1]^+$ 368.4 (calculated for $C_{20}H_{33}NO_5$, 368.2). ^{1}H NMR (CD_3OD): δ 5.43 (s, 1H), 5.23 (t, 1H), 3.70 (m, 1H), 3.66 (dd, 1H), 3.43 (s, 3H), 2.96 (d, 1H), 2.61 (t, 1H), 2.56 (d, 1H), 2.31 (m, 1H), 2.19 (m, 1H), 2.10 (dt, 1H), 1.94 (d, 1H), 1.90 (m, 1H), 1.82 (m, 1H), 1.75 (s, 3H), 1.67 (s, 3H), 1.19 (s, 3H), 1.13 (d, 6H), 1.05 (m, 1H).

(3*R*,4*S*,5*S*,6*R*)-5-Methoxy-4-((2*R*,3*R*)-2-methyl-3-(3-methylbut-2-enyl)oxiran-2-yl)-1-oxaspiro[2.5]octan-6-yl *tert*-Butylcarbamate (24). General procedure B was followed. LRMS (*m*/*z*) $[M + 1]^+$ 382.3 (calculated for $C_{21}H_{35}NO_5$, 382.2). ^{1}H NMR (CD_3OD): δ 5.37 (s, 1H), 5.23 (t, 1H), 3.65 (dd, 1H), 3.41 (s, 3H), 2.95 (d, 1H), 2.62 (t, 1H), 2.55 (d, 1H), 2.31 (m, 1H), 2.22 (m, 1H), 2.10 (dt, 1H), 1.96 (d, 1H), 1.92 (m, 1H), 1.80 (m, 1H), 1.75 (s, 3H), 1.67 (s, 3H), 1.29 (s, 9 H), 1.19 (s, 3H), 1.04 (m, 1H).

1-Oxaspiro[2.5]octane (25). To a solution of MCPBA (5.6 g, 32.6 mmol) in $CHCl_3$ was added dropwise methylene cyclohexane (3.75 mL, 31 mmol). The mixture was stirred 16 h at 4 °C, after which the chloroform was partially evaporated under a nitrogen stream. The residue was taken up in ether (50 mL) and washed with sodium bicarbonate. The product was purified by distillation (bp 70 °C), yield 1.24 g (34%). LRMS (*m*/*z*) $[M + 1]^+$ 113.1 (calculated for $C_7H_{12}O$, 113.1). ^{1}H NMR (CD_3OD): δ 2.59 (s, 2H), 1.68 (m, 2H), 1.60 (m, 2H), 1.58 (m, 2H), 1.50 (m, 2H), 1.46 (m, 2H). ^{13}C NMR (CD_3OD): δ 54.1 (CH_2), 59.1 (C), 33.3 (CH_2), 24.6 (CH_2), 25.0 (CH_2), assigned by HSQC.

Molecular Modeling. Binding poses were generated using the program MOE (Chemical Computing Group) together with the cocrystal structure of human MetAP2 with fumagillin (1BOA).[4]

MetAP-2 Inhibition. Compounds were prepared as 800 nM solutions in reaction buffer (1% glycerol, 20 mM HEPES, 100 mM KCl, 0.1 mM $CoSO_4$) and combined with equal volumes of 80 nM $MetAP_2$. Samples were taken in triplicate at 1, 2, 4, and 8 h time points and treated with 2× Met-AMC substrate to determine residual activity. Final concentrations of MetAP2 and compound were 20 and 200 nM, respectively.

HUVEC Assay. Human umbilical vein endothelial cells (HUVEC) were cultured in HUVEC growth medium (Clonetics) at 37 °C. For proliferation assays, 2000 cells (20000 cells/mL) (passage 3−5) were seeded in 96-well plates (in triplicate). After cell attachment, fresh medium containing **8** was added for 72 h. To each well, 0.25 mg per mL of MTT was added, and the plates were incubated for 2 h at 37 °C. The MTT was removed, and the crystals were solubilized with isopropyl alcohol. After 10 min, the intensity was measured colorimetrically at a wavelength of 570 nm. HUVEC proliferation was determined by the conversion of MTT to water-insoluble MTT-formazan by mitochondrial dehydrogenases of living cells.

BAEC Assay. The bovine aortic endothelial growth assay was performed as described by Turk et al.[7a]

Cassette PK Study. Two groups of 8 male Sprague−Dawley rats (aged 8−9 weeks, Taconic) were dosed with multiple compounds at 10 mg/kg compound (po) or 5 mg/kg (iv), respectively, in 5% HPCD formulation containing 2 mg/mL compound. Approximately 0.5 mL of blood was drawn by jug stick from four animals at alternating time points as follows: 2 min, 5 min, 10 min, 15 min, 30 min, 60 min, 2 h, 4 h, 6 h. Samples were treated with EDTA, centrifuged, and frozen. Compounds were quantitated from plasma samples by LCMS.

Acknowledgment. We thank Dr. Sylvie Bernier for her thoughtful review of the manuscript.

References

(1) (a) DiPaolo, J. A.; Tarbell, D. S.; Moore, G. E. Studies on the carcinolytic activity of fumagillin and some of its derivatives. *Antibiot. Annu.* **1958−1959**, *6*, 541–546. (b) Ingber, D.; Fujita, T.; Kishimoto, S.; Sudo, K.; Kanamaru, T.; Brem, H.; Folkman, J.

Synthetic analogues of fumagillin that inhibit angiogenesis and suppress tumor growth. *Nature* **1990**, *348*, 555–557.
(2) (a) Folkman, J. Angiogenesis: an organizing principle for drug discovery? *Nature Rev. Drug Discovery* **2007**, *6*, 273–286. (b) Ribatti, D. The discovery of antiangiogenic molecules: a historical review. *Curr. Pharm. Des.* **2009**, *15*, 345–352.
(3) (a) Sin, N.; Meng, L.; Wang, M. Q. W.; Wen, J. J.; Bornmann, W. G.; Crews, C. M. The anti-angiogenic agent fumagillin covalently binds and inhibits the methionine aminopeptidase, MetAP-2. *Proc. Natl. Acad. Sci. U.S.A.* **1997**, *94*, 6099–6103. (b) Griffith, E. C.; Su, Z.; Turk, B. E.; Chen, S.; Chang, Y.-H.; Wu, Z.; Biemann, K.; Liu, J. O. Methionine aminopeptidase (type 2) is the common target for angiogenesis inhibitors AGM-1470 and ovalicin. *Chem. Biol.* **1997**, *4*, 461–471.
(4) Liu, S.; Widom, J.; Kemp, C. W.; Crews, C. M.; Clardy, J. Structure of human methionine aminopeptidase-2 complexed with fumagillin. *Science* **1998**, *282*, 1324–1327.
(5) Griffith, E. C.; Su, Z.; Niwayama, S.; Ramsay, C. A.; Chang, Y.-H.; Liu, J. O. Molecular recognition of angiogenesis inhibitors fumagillin and ovalicin by methionine aminopeptidase 2. *Proc. Natl. Acad. Sci. U.S.A.* **1998**, *95*, 15183–15188.
(6) (a) Marui, S.; Itoh, F.; Kozai, Y.; Sudo, K.; Kishimoto, S. Chemical Modification of Fumagillin. I. 6-*O*-Acyl, 6-*O*-Alkyl, and 6-*O*-(*N*-Substituted-carbamoyl)fumagillols. *Chem. Pharm. Bull.* **1992**, *40*, 96–101. (b) Bernier, S. G.; Westlin, W. F.; Hannig, G. Fumagillin class inhibitors of methionine aminopeptidase-2. *Drugs Future* **2005**, *30*, 497–508. (c) Lee, H.; Cho, C.; Kang, S.; Yoo, Y.; Shin, J.; Ahn, S. Design, synthesis, and antioangiogenic effects of a series of potent novel fumagillin analogues. *Chem. Pharm. Bull.* **2007**, *55*, 1024–1029. (d) Zhong, H.; Bowen, J. P. Antiangiogenesis drug design: multiple pathways targeting tumor vasculature. *Curr. Med. Chem.* **2006**, *13*, 849–862. (e) Folkman, J. Tumor angiogenesis. In *Accomplishments in Cancer Research 1997*; Wells, S. A., Sharp, P. A., Eds.; Lippincott Williams & Wilkins: Philadelphia, 1998; pp 32−44. (f) Lefkove, B.; Govindarajan, B.; Arbiser, J. Fumagillin: an anti-infective as a parent molecule for novel angiogenesis inhibitors. *Expert Rev. Anti-Infect. Ther.* **2007**, *5*, 573–579.
(7) (a) Turk, B.; Griffith, E.; Wolf, S.; Biemann, K.; Chang, Y.-H.; Liu, J. Selective inhibition of amino-terminal methionine processing by TNP-470 and ovalicin in endothelial cells. *Chem. Biol.* **1999**, *11*, 823–833. (b) Zhang, Y.; Griffith, E. C.; Sage, J.; Jacks, T.; Liu, J. O. Cell cycle inhibition by the anti-angiogenic agent TNP-470 is mediated by p53 and $p^{21WAF1/CIP1}$. *Proc. Natl. Acad. Sci. U.S.A.* **2000**, *97*, 6427–6432.
(8) Bernier, S. G.; Taghizadeh, N.; Thompson, C. D.; Westlin, W. F.; Hannig, G. Methionine aminopeptidases type I and type II are essential to control cell proliferation. *J. Cell. Biochem.* **2005**, *95*, 1191–1203.
(9) Hu, X.; Dang, Y.; Tenney, K.; Crews, P.; Tsai, C.; Sixt, K.; Cole, P.; Liu, J. Regulation of c-Src nonpeptide tyrosine kinase activity by bengamide A through inhibition of methionine aminopeptidases. *Chem. Biol.* **2007**, *14*, 764–774.
(10) (a) Peacock, D. J.; Banquerigo, M. L.; Brahn, E. Angiogenesis inhibition suppresses collagen arthritis. *J. Exp. Med.* **1992**, *175*, 1135–1138. (b) Oliver, S. J.; Banquerigo, M. L.; Brahn, E. Suppression of collagen induced arthritis using an angiogenesis inhibitor, AGM-1470, and a microtubule stabilizer, Taxol. *Cell. Immunol.* **1994**, *157*, 291–299. (c) Peacock, D. J.; Banquerigo, M. L.; Brahn, E. A novel angiogenesis inhibitor suppresses rat adjuvant arthritis. *Cell. Immunol.* **1995**, *160*, 178–184. (d) Oliver, S. J.; Cheng, T. P.; Banquerigo, M. L.; Brahn, E. Suppression of collagen-induced arthritis by an angiogenesis inhibitor, AGM-1470, in combination with cyclosporin: reduction of vascular endothelial growth factor (VEGF). *Cell. Immunol.* **1995**, *166*, 196–206.
(11) (a) Kudelka, A. P.; Levy, T.; Verschraegen, C. F.; Edwards, S. P.; Termrungruanglert, W.; Freedman, R. S.; Kaplan, A. L.; Kieback, D. G.; Meyers, C. A.; Jaeckle, K. A.; Loyer, E.; Steger, M.; Mante, R.; Mavligit, G.; Killian, A.; Tang, R. A.; Gutterman, J. U.; Kavanagh, J. J. A phase I study of TNP-470 administered to patients with advanced squamous cell cancer of the cervix. *Clin. Cancer Res.* **1997**, *3*, 1501–1505. (b) Figg, W. D.; Pluda, J. M.; Lush, R. M.; Saville, M. W.; Wyvill, K.; Reed, E.; Yarchoan, R. The pharmacokinetics of TNP-470, a new angiogenesis inhibitor. *Pharmacotherapy* **1997**, *17*, 91–97. (c) Dezube, B. J.; Van Roenn, J. H.; Holden-Wiltse, J.; Cheung, T. W.; Remick, S. C.; Cooley, T. P.; Moore, J.; Sommadossi, J.-P.; Shriver, S. L.; Suckow, C. W.; Gill, P. S. Fumagillin analog in the treatment of Kaposi's sarcoma: a phase I AIDS clinical trial group study. *J. Clin. Oncol.* **1998**, *16*, 1444–1449. (d) Bhargava, P.; Marshall, J. L; Rizvi, N.; Dahut, W.; Yoe, J.; Figuera, M.; Phipps, K.; Ong, V. S.; Kato, A.; Hawkins, M. J. A phase I and pharmacokinetic study of TNP-470 administered weekly to patients with advanced cancer. *Clin. Cancer Res.* **1999**, *5*, 1989–1995. (e) Stadler, W. M.; Kuzel, T.; Shapiro, C.; Sosman, J.; Clark, J.; Vogelzang, N. J. Multi-Institutional Study of the Angiogenesis Inhibitor TNP-470 in Metastatic Renal Carcinoma. *J. Clin. Oncol.* **1999**, *17*, 2541–2545. (f) Moore, J. D.; Dezube, B. J.; Gill, P.; Zhou, X.-J.; Acosta, E. P.; Sommadossi, J.-P. Phase I dose escalation pharmacokinetics of O-(chloroacetylcarbamoyl)-fumagillin (TNP-470) and its metabolites in AIDS patients with Kaposi's sarcoma. *Cancer Chemother. Pharmacol.* **2000**, *46*, 173–179. (g) Logothetis, C. J.; Wu, K. K.; Finn, L. D.; Daliani, D.; Figg, W.; Ghaddar, H.; Gutterman, J. U. Phase I trial of the angiogenesis inhibitor TNP-470 for progressive androgen-independent prostate cancer. *Clin. Cancer Res.* **2001**, *7*, 1198–1203.
(12) (a) Moore, J. D.; Sommadossi, J.-P. ACTG 215 Study Team. Determination of *O*-(chloroacetylcarbamoyl)fumagillol (TNP-470; AGM-1470) and two metabolites in plasma by high-performance liquid chromatography/mass spectrometry with atmospheric pressure chemical ionization. *J. Mass Spectrom.* **1995**, *30*, 1707–1715. (b) Placidi, L.; Cretton-Scott, E.; De Sousa, G.; Rahmani, R.; Placidi, M.; Sommadossi, J.-P. Disposition and metabolism of the angiogenic moderator O-(chloroacetyl-carbamoyl) fumagillol (TNP-470; AGM-1470) in human hepatocytes and tissue microsomes. *Cancer Res.* **1995**, *55*, 3036–3042.
(13) (a) Satchi-Fainaro, R.; Puder, M.; Davies, J. W.; Tran, H. T.; Sampson, D. A.; Greene, A. K.; Corfas, G.; Folkman, J. Targeting angiogenesis with a conjugate of HPMA copolymer and TNP-470. *Nature Med.* **2004**, *10*, 255–261. (b) Satchi-Fainaro, R.; Mamluk, R.; Wang, L.; Short, S. M.; Nagy, J. A.; Feng, D.; Dvorak, A. M.; Dvorak, H. F.; Puder, M.; Mukhopadhyay, D.; Folkman, J. Inhibition of vessel permeability by TNP-470 and its polymer conjugate, caplostatin. *Cancer Cell* **2005**, *7*, 251–261. (c) Benny, O.; Fainaru, O.; Adini, A.; Cassiola, F.; Bazinet, L.; Adini, I.; Pravda, E.; Nahmias, Y.; Koirala, S.; Corfas, G.; D'Amato, R. J.; Folkman, J. An orally delivered small-molecule formulation with antiangiogenic and anticancer activity. *Nat. Biotechnol.* **2008**, *26*, 799–807.
(14) (a) Han, C. K.; Ahn, S. K.; Choi, N. S.; Hong, R. K.; Moon, S. K.; Chun, H. S.; Lee, S. J.; Kim, J. W.; Hong, C. I.; Kim, D.; Yoon, J. H.; No, K. T. Design and synthesis of highly potent fumagillin analogues from homology modeling for a human MetAP-2. *Bioorg. Med. Chem. Lett.* **2000**, *10*, 39–43. (b) Jeong, B.-S.; Choi, N. S.; Ahn, S. K.; Bae, H.; Kim, H. S.; Kim, D. Total synthesis and antiangiogenic activity of cyclopentane analogues of fumagillol. *Bioorg. Med. Chem. Lett.* **2005**, *15*, 3580–3583. (c) Kim, E.-J.; Shin, W.-H. General pharmacology of CKD-732, a new anticancer agent: effects on central nervous, cardiovascular, and respiratory system. *Biol. Pharm. Bull.* **2005**, *28*, 217–223. (d) Lee, H. W.; Cho, C. S.; Kang, S. K.; Yoo, Y. S.; Shin, J. S.; Ahn, S. K. Design, synthesis, and antiangiogenic effects of a series of potent novel fumagillin analogues. *Chem. Pharm. Bull.* **2007**, *55*, 1024–1029. (e) Rodeschini, V.; Boiteau, J.-G.; Van de Weghe, P.; Tarnus, C.; Eustache, J. MetAP-2 inhibitors based on the fumagillin structure. Side-chain modification and ring-substituted analogues. *J. Org. Chem.* **2004**, *69*, 357–373. (f) Rodeschini, V.; Van de Weghe, P.; Salomon, E.; Tarnus, C.; Eustache, J. Enantioselective approaches to potential MetAP-2 reversible inhibitors. *J. Org. Chem.* **2005**, *70*, 2409–2412. (g) Rodeschini, V.; Van de Weghe, P.; Tarnus, C.; Eustache, J. A Simple spiroepoxide as methionine aminopeptidase-2 inhibitor: synthetic problems and solutions. *Tetrahedron Lett.* **2005**, *46*, 6691–6695. (h) Baldwin, J. E.; Bulger, P. G.; Marquez, R. Fast and efficient synthesis of novel fumagillin analogues. *Tetrahedron* **2002**, *58*, 5441–5452. (i) Pyun, H.-J.; Fardis, M.; Tario, J.; Yang, C. Y.; Ruckman, J.; Henninger, D.; Jin, H.; Kim, C. U. Investigation of novel fumagillin analogues as angiogenesis inhibitors. *Bioorg. Med. Chem. Lett.* **2004**, *14*, 91–94. (j) Mazitschek, R.; Huwe, A.; Giannis, A. Synthesis and biological evaluation of novel fumagillin and ovalicin analogues. *Org. Biomol. Chem.* **2005**, *3*, 2150–2154.
(15) Olson, G. L.; Self, C.; Lee, L.; Cook, C. M.; Birktoft, J. J. U.S. Patent 6,548,477, April 15, **2003**.
(16) (a) Kendall, R. L.; Bradshaw, R. A. Isolation and characterization of the methionine aminopeptidase from porcine liver responsible for the co-translational processing of proteins. *J. Biol. Chem.* **1992**, *267*, 20667–20673. (b) Zuo, S.; Guo, O.; Ling, C.; Chang, Y.-H. Evidence that two zinc fingers in the methionine aminopeptidase from Saccharomyces cerevisiae are important for normal growth. *Mol. Gen. Genet.* **1995**, *246*, 247–253.
(17) (a) Zhou, G.; Tsai, C. W.; Liu, J. O. Fumagalone, a reversible inhibitor of type 2 methionine aminopeptidase and angiogenesis. *J. Med. Chem.* **2003**, *46*, 3452–3454. (b) Lu, J.; Chong, C. R.; Hu, X.; Liu, J. O. Fumarranol, a rearranged fumagillin analogue that inhibits angiogenesis in vivo. *J. Med. Chem.* **2006**, *49*, 5645–5648.
(18) Bernier, S. G.; Lazarus, D. D; Clark, E.; Doyle, B.; Labenski, M. T.; Thompson, C. D.; Westlin, W. F.; Hannig, G. A methionine aminopeptidase-2 inhibitor, PPI-2458, for the treatment of rheumatoid arthritis. *Proc. Natl. Acad. Sci. U.S.A.* **2004**, *101*, 10768–10773.

(19) (a) Cooper, A. C.; Karp, R. M.; Clark, E. J.; Taghizadeh, N. R.; Hoyt, J. G.; Labenski, M. T.; Murray, M. J.; Hannig, G.; Westlin, W. F.; Thompson, C. D. A novel methionine aminopeptidase-2 inhibitor, PPI-2458, inhibits Non-Hodgkin's lymphoma cell proliferation in vitro and in vivo. *Clin. Cancer Res.* **2006**, *12*, 2583–2590. (b) Hannig, G.; Lazarus, D. D.; Bernier, S. G.; Karp, R. M.; Lorusso, J.; Qiu, D.; Labenski, M. T.; Wakefield, J. D.; Thompson, C. D.; Westlin, W. F. Inhibition of melanoma tumor growth by a pharmacological inhibitor of MetAP-2, PPI-2458. *Int. J. Oncol.* **2006**, *28*, 955–963.

(20) (a) Brahn, E.; Banquerigo, M. L.; Schoettler, N. R.; Lee, S. A new antiangiogenesis inhibitor, PPI-2458: regression of collagen-induced arthritis and prevention of erosions. *Arthritis Rheum.* **2001**, *44*, S271. (b) Brahn, E.; Schoettler, N. R.; Banquerigo, M. L.; Thompson, C. D. Involution of collagen-induced arthritis with angiogenesis inhibitor PPI-2458. *Arthritis Rheum.* **2003**, *48*, S347. (c) Hannig, G.; Bernier, S. G.; Hoyt, J. G.; Doyle, B.; Clark, E.; Karp, R. M.; Lorusso, J.; Westlin, W. F. Suppression of inflammation and structural damage in experimental arthritis through molecular targeted therapy with PPI-2458. *Arthritis Rheum.* **2007**, *56*, 850–860. (d) Lazarus, D. D.; Doyle, E. G.; Bernier, S. G.; Rogers, A. B.; Labenski, M. T.; Wakefield, J. D.; Karp, R. M.; Clark, E. J.; Lorusso, J.; Hoyt, J. G.; Thompson, C. D.; Hannig, G.; Westlin, W. F. An inhibitor of methionine aminopeptidase type-2, PPI-2458, ameliorates the pathophysiological disease processes of rheumatoid arthritis. *Inflamm. Res.* **2008**, *57*, 18–27. (e) Bainbridge, J.; Madden, L.; Essex, D.; Binks, M.; Malhotra, R.; Paleolog, E. M. Methionine aminopeptidase-2 blockade reduces chronic collagen-induced arthritis: potential role for angiogenesis inhibition. *Arthritis Res. Ther.* **2007**, *9*, R127.